ARL-TR-9595 ● Oct 2022

DEVCOM ARMY RESEARCH LABORATORY

# Analysis of Thermal Stability of Morphology in Certain Polymers Using X-ray Scattering

by Frederick L Beyer and Randy A Mrozek

## NOTICES

### Disclaimers

The findings in this report are not to be construed as an official Department of the Army position unless so designated by other authorized documents.

Citation of manufacturer's or trade names does not constitute an official endorsement or approval of the use thereof.

Destroy this report when it is no longer needed. Do not return it to the originator.

ARL-TR-9595 ● OCT 2022


# Analysis of Thermal Stability of Morphology in Certain Polymers Using X-ray Scattering

**Frederick L Beyer and Randy A Mrozek**
*DEVCOM Army Research Laboratory*

# REPORT DOCUMENTATION PAGE

*Form Approved*
*OMB No. 0704-0188*



| 1. REPORT DATE *(DD-MM-YYYY)* | 2. REPORT TYPE | 3. DATES COVERED (From - To) |
|---|---|---|
| October 2022 | Technical Report | 1 October 2021 – 6 September 2022 |

**4. TITLE AND SUBTITLE**
Analysis of Thermal Stability of Morphology in Certain Polymers Using X-ray Scattering

**5a. CONTRACT NUMBER**

**5b. GRANT NUMBER**

**5c. PROGRAM ELEMENT NUMBER**

**6. AUTHOR(S)**
Frederick L Beyer and Randy A Mrozek

**5d. PROJECT NUMBER**

**5e. TASK NUMBER**

**5f. WORK UNIT NUMBER**

**7. PERFORMING ORGANIZATION NAME(S) AND ADDRESS(ES)**
DEVCOM Army Research Laboratory
ATTN: FCDD-RLW-MG
Aberdeen Proving Ground, MD 21005

**8. PERFORMING ORGANIZATION REPORT NUMBER**
ARL-TR-9595

**9. SPONSORING/MONITORING AGENCY NAME(S) AND ADDRESS(ES)**

**10. SPONSOR/MONITOR'S ACRONYM(S)**

**11. SPONSOR/MONITOR'S REPORT NUMBER(S)**

**12. DISTRIBUTION/AVAILABILITY STATEMENT**
Approved for public release: distribution unlimited.

**13. SUPPLEMENTARY NOTES**
ORCID ID: Frederick L Beyer, 0000-0003-0253-2134

**14. ABSTRACT**

In this study, X-ray scattering was combined with in situ heating to at least 200 °C to determine the morphological stability of a series of thermoplastics typically used in high-temperature applications. Poly(phenyl sulfone) (PPSU), poly(ether imide) (PEI), and a proprietary blend based primarily on polycarbonate (PC) showed the best thermal stability. Samples of poly(oxymethylene) (POM), poly(p-phenylene sulfide) (PPS), impact-modified high-temperature nylon, and filled high-temperature nylon all exhibited changes in morphology as a function of temperature. POM exhibited strong crystallinity at room temperature and displayed a sharp melting transition around 170 °C, becoming a free-flowing liquid. The small-angle X-ray scattering data indicate that the POM crystallites begin to change as early as 130 °C. In contrast, PPS crystallized upon heating, at approximately 105 °C. PPS was found to be morphologically unstable at only 70 °C. The results from this study suggest that PPSU, PEI, and the PC-siloxane product studied here may be considered thermally stable under these testing conditions.

**15. SUBJECT TERMS**
Sciences of Extreme Materials, X-ray scattering, poly(p-phenylene sulfide), poly(phenyl sulfone), thermal stability, invariant

| 16. SECURITY CLASSIFICATION OF: | | | 17. LIMITATION OF ABSTRACT | 18. NUMBER OF PAGES | 19a. NAME OF RESPONSIBLE PERSON |
|---|---|---|---|---|---|
| a. REPORT | b. ABSTRACT | c. THIS PAGE | | | Frederick L Beyer |
| Unclassified | Unclassified | Unclassified | UU | 27 | 19b. TELEPHONE NUMBER (Include area code) (410) 306-0893 |

Standard Form 298 (Rev. 8/98)
Prescribed by ANSI Std. Z39.18

## Contents

## List of Figures

## List of Tables

## Acknowledgments

Frederick L Beyer wishes to thank JL Lenhart for helpful conversations regarding the thermal behavior of poly(phenylene sulfone).

## 1. Introduction

Small-angle X-ray scattering (SAXS) and wide-angle X-ray scattering (WAXS) are nondestructive techniques providing information on the internal structure of materials. Information on crystallinity, microphase separation, microphase-separated domain size and shape, and long-range order is often determined using SAXS and WAXS.[1,2] When combined with in situ sample manipulation[3] such as polymerization,[4] heating,[5] mechanical deformation,[6] rheology,[7] or changes in environmental conditions,[8] time-resolved X-ray scattering techniques can give insight into the overall usefulness of materials under challenging environments.

In this report, the findings of a study exploring the effect of heating on a series of polymers, including primarily poly(oxymethylene) (POM) and poly(p-phenylene sulfide) (PPS), are presented. These polymers were all chosen for their high-temperature performance characteristics, including mechanical strength, heat-deflection behavior, glass transition temperature ($T_g$), and melting temperature ($T_m$) when applicable. The desired material should be stable at temperatures exceeding 100 °C for short periods of time and capable of long-term storage without degradation at temperatures up to 70 °C. SAXS and WAXS were used to study the effect of heating on these materials, and any change in morphology was taken as a sign of potential instability. The US Army commonly requires maintaining a minimum 20-year lifetime under broad storage environments. Even subtle changes to the polymer can lead to substantial performance changes over extended time periods.

## 2. Experimental

A range of commercial materials was acquired for these measurements. Table 1 lists the materials studied along with density, $T_g$, $T_m$, and heat-deflection temperature (HDT). The data in Table 1 are taken from materials information sheets provided by manufacturers except for those in parentheses, which are general values from the literature.[9,10]

**Table 1 Summary information for materials tested in this study**

| Name | Trade name examples | Product tested | Density ($g/cm^3$) | $T_m$ (°C) | $T_g$ (°C) | HDT (°C)[a] |
|---|---|---|---|---|---|---|
| Poly(oxymethylene) (POM) | Delrin, Iupital, Acetal | Iupital F20 | 1.41 | 165 | . . . | 110 |
| Polycarbonate (PC) | Lexan, Makrolon | Lexan 1414T[b] | 1.19 | N/A | (147) | 116, 120[c] |
| Poly(phenyl sulphone) (PPSU) | Radel | Radel 5800 | 1.29 | N/A | 220 | 207 |
| Poly(ether imide) (PEI) | Ultem | Ultem 1000 | 1.27 | (300–320) | . . . | 190,192, 201[d] |
| Poly(p-phenylene sulfide) (PPS) | Ryton, Fortron, Tedur, Supec | Proprietary | (1.35) | (285) | (75–85) | (120–130) |
| Impact-modified high-temperature nylon (HTN-IM) | Zytel, Celanese, Ultramid | Zytel FE8200 | 1.13 | 300 | . . . | 125 |
| Filled high-temperature nylon (F-HTN) | Zytel, Celanese, Ultramid | Zytel 50G35 FWS | 1.47 | 299 | . . . | . . . |

[a] Measured with 1.8-MPa load.
[b] Lexan Copolymer EXL1414T is a copolymer of PC and "siloxane."
[c] ASTM D648[11] and ISO 75/Af,[12] respectively.
[d] ASTM D648 3.2 mm, ISO 75/Af, ASTM D648 6.4 mm, respectively.

X-ray scattering data (both SAXS and WAXS) were collected using a Xenocs SAXS instrument, model Xeuss 3.0 HR. X-rays were generated with a Rigaku MicroMax-007HF rotating copper anode X-ray generator operated at 40 kV and 30 mA. Characteristic $Cu_{K\alpha}$ photons were monochromated and collimated using a focusing optic and two scatterless slit apertures, producing a well-aligned incident beam with wavelength ($\lambda$) of 1.5418 Å. Data were collected using a Dectris PilatusR 300k solid-state X-ray detector. Isotropic 2-D data were azimuthally averaged to generate 1-D data, $I(q)$, for analysis. Silver behenate was used to calibrate the beam center and sample-to-detector distance.[13] Transmitted flux was used to place-correct the data for absorption, but without thickness measurements the data could not be placed on an absolute scale. In general, the data were not corrected for instrumental background, which in this case originates almost exclusively from the sample holders. Data processing and analysis were performed using Wavemetrics Igor Pro v8 and procedures available from Argonne National Laboratory.[14]

In situ heating was performed using a Linkam HFSX350 heating stage. Samples were cut into discs 6 mm in diameter and roughly 1 mm thick, then mounted in stainless steel sandwich cells equipped with mica windows 6 μm thick. The

sandwich cells were mounted on the heating block and placed under vacuum in the sample chamber for measurement. Samples were heated at no more than 1 °C/min, starting between 20 and 25 °C. Temperature was calibrated using an indium foil standard.

Several different detector positions and sample-to-detector distances (SDDs) were used during the heating cycles. A typical experiment involved setting the point of normal incidence near the detector center and collecting data at 370 mm SDD, giving an angular range of 0.02 $Å^{-1} < q < 0.7$ $Å^{-1}$, where $q$ is the modulus of the scattering vector, such that $q = 4\pi \sin(\theta)/\lambda$, where $2\theta$ is the scattering angle. To collect wide-angle data, the detector was periodically moved to an SDD of 55 mm, providing data up to approximately 3 $Å^{-1}$. A custom configuration, in which the detector was repositioned so that the point of normal incidence was positioned in a corner of the detector and the SDD was set to approximately 200 mm, was used to span most of the SAXS and WAXS range of interest simultaneously.

## 3. Results and Discussion

### 3.1 Poly(oxymethylene)

The first material characterized was POM, a semicrystalline polymer with two well-established molecular arrangements of either the trigonal or orthorhombic crystal structures having the P3 and P222 space groups, respectively.[15,16] Room-temperature wide-angle scattering data best match the orthorhombic structure with lattice parameters of 4.767, 7.660, and 3.563 Å. The weak peak at 1.4 $Å^{-1}$ is the (100) reflection, while the stronger peak at 1.6 $Å^{-1}$ is a combination of diffraction from the (110), (020), and (001) planes. The peak at 2.38 $Å^{-1}$ is a combination of the (111) and (210) reflections. The diffraction peaks are significantly broadened due to the thickness of the sample and suggest that the sample is not highly crystalline.

Figure 1A shows the results of in situ heating of POM during WAXS measurements. Prior to approximately 130 °C, little change was observed. Above 130 °C, the Bragg diffraction peaks disappear completely at approximately 170 °C, slightly lower than the reported values for Delrin 150 (181 °C), extended chain fibers (182.5 °C), and folded chain crystallites (174 °C). However, copolymers of methylene glycol and other monomers can have significantly lower melting points, suggesting that Iupital F20 is a copolymer of oxymethylene and some other monomer.[15]

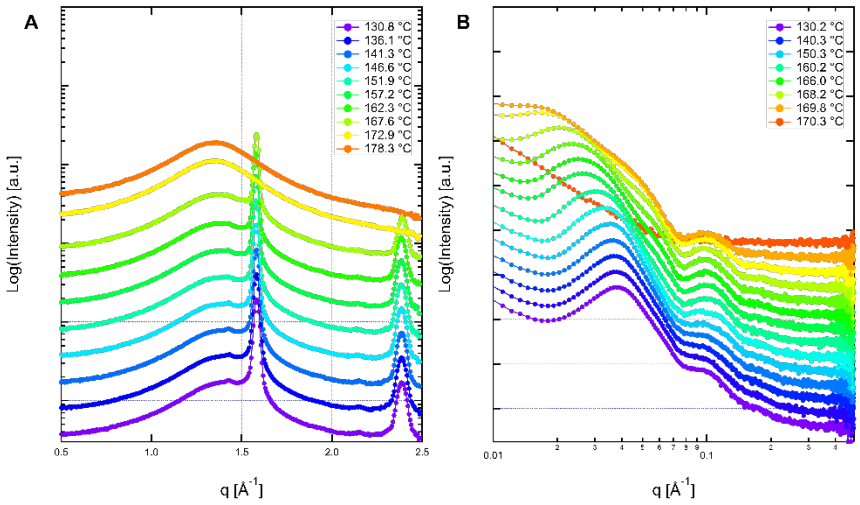


**Fig. 1 A) WAXS data for POM during heating. Data are shown from 131 to 178 °C and reveal a sharp melting transition at approximately 168 °C. B) SAXS data collected during heating of POM sample, showing changes in form factor scattering as the crystallites melt. Data are shown from 130 to 160 °C in 10 °C increments, and from 166 to 170 °C in 2 °C increments. In both A and B, the data are shifted vertically for clarity.**

Figure 1B shows the SAXS data collected simultaneously with the WAXS data. The data show a combination of a strong correlation peak arising from the regular structure of the lamellar crystallites and weaker form factor features arising from the discotic shape of the crystallites.[15] The primary SAXS reflection is centered at 0.04 $Å^{-1}$, corresponding to a regular spacing of 15.7 nm between crystalline lamellae (center-to-center distance). In addition to the loss of structure observed around 170 °C, the SAXS data show a morphological transition that accelerates as the sample temperature approaches $T_m$. The correlation peak at 0.04 $Å^{-1}$ shifts to lower angles, reaching approximately 0.02 $Å^{-1}$ before the crystallites melt. This indicates that the crystallites are, on average, moving apart from one another. This process is slow at first but accelerates around 160 °C, likely corresponding to melting of smaller crystallites, a process that would lead to an increasingly large separation between domains. The higher order features in the SAXS data, such as the form factor fringe at 0.1 $Å^{-1}$, remain clear and shift slightly to higher angles, suggesting a reduction in the size of the individual crystallites with increasing temperatures. Between 168 and 170 °C, the scattering from the polymer vanishes, leaving only scattering from the sample cell, indicating that the sample liquified and flowed out of the path of the X-ray beam. Visual inspection of the sandwich cell after the experiment confirmed the physical change in sample shape.

## 3.2 Poly(p-phenylene sulfide)

PPS samples were taken from specimens provided by a vendor. The vendor did not provide any additional information on the specific PPS product used. PPS is known for its thermal stability and high-temperature performance with a $T_m$ of 285 °C.[9] The HDT (1.8 MPa load) is approximately 125 °C but can be increased substantially by the addition of rigid fillers such as glass fibers. The $T_g$ of PPS is only approximately 80 °C, however.

Room temperature SAXS and WAXS data revealed no morphological features of note. Only an amorphous halo in the WAXS region and a typical power-law background in the SAXS region were observed, as indicated by the purple (room temperature) traces in Fig. 2. Upon heating, the PPS crystallizes around 105 °C. In the WAXS data (Fig. 2A), this is manifest as the appearance of Bragg diffraction peaks superimposed on the amorphous halo, starting at roughly 1.4 $Å^{-1}$. These diffraction peaks are not sharp, indicating the formation of relatively small crystallites.

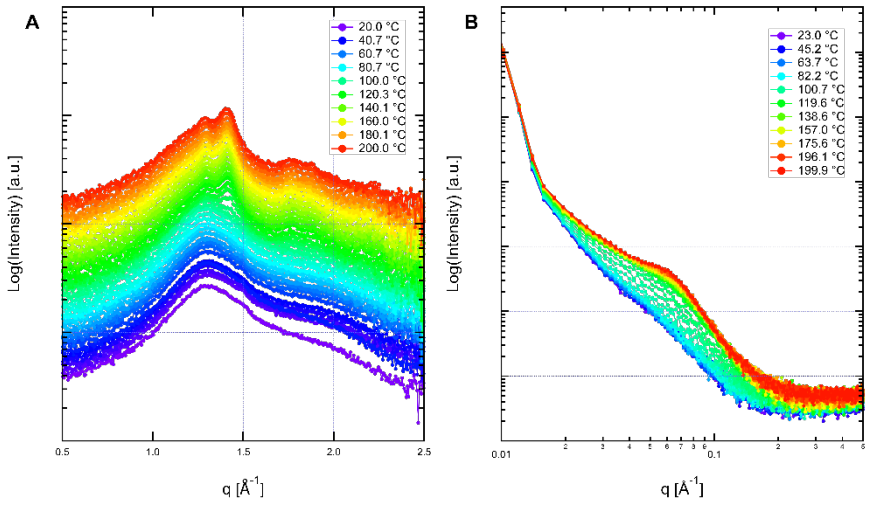


**Fig. 2 A) WAXS data for PPS heated from 20 to 200 °C. Crystallization resulting in Bragg diffraction occurs around 105 °C. WAXS data are scaled vertically for clarity. B) SAXS data collected for PPS when heated from 20 to 200 °C. A feature emerges in the SAXS data beginning around 80 °C.**

Figure 2B shows the SAXS data collected during the in situ heating experiment. An ill-defined feature emerges beginning around 80 °C and continues increasing in intensity, not quite reaching a steady state at 200 °C. This feature is a correlation peak arising from interdomain scattering between PPS crystallites. At temperatures between 80 and 105 °C, the intensity of the correlation peak represents correlation between emerging density fluctuations in the material that evolve into crystallization.

The observation of a relevant morphological change at 80 °C required further exploration. In particular, a reasonable question is whether or not the material is stable at lower temperatures given a requirement of potentially long-term storage at temperatures approaching 70 °C. To probe this behavior, a sample of PSS was heated to 70 °C and annealed for over 100 h while collecting scattering data at a position chosen to allow spanning both the SAXS and WAXS regimes simultaneously. In these data, shown in Fig. 3, it is apparent visually that the same increase in the SAXS regime observed in Fig. 2 at 80 °C and higher is occurring during annealing at 70 °C.

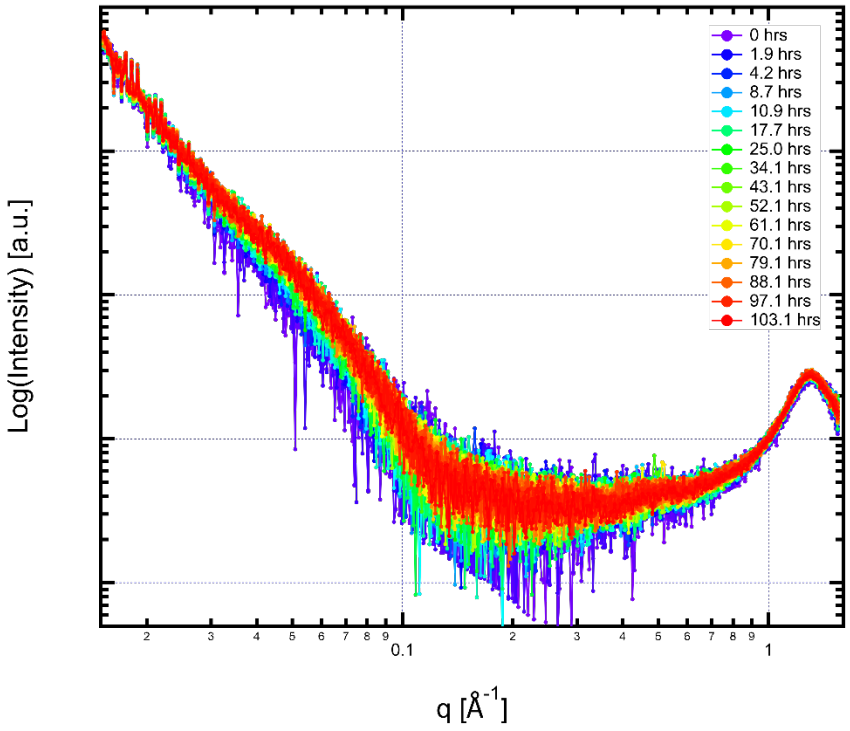


**Fig. 3 SAXS and WAXS data collected for PPS with in situ annealing at 70 °C for 103 h. A change is observed in the low-angle feature.**

To quantify the emergence of the correlation feature in the SAXS data, the Porod Invariant was calculated from the SAXS data.[1,2] The Porod Invariant ($Q$) is a measure of the overall scattering from a sample.

$$Q = \frac{1}{2\pi^2} \int_{q=0}^{\infty} I(q) q^2 \, dq = V(\rho_1 - \rho_2)^2 \phi_1 \phi_2 \qquad (1)$$

The invariant is calculated by integrating the scattered intensity, $I(q)$, times the scattering vector magnitude squared, $q^2$. Although the integration is from $q = 0$ to $q = \infty$, in practice the integration need not exceed $q = 0.3$ Å$^{-1}$, and the data in the

low-$q$ region can be approximated as a constant. The method used for calculating the invariant was described previously.[18]

In a two-phase material, $Q$ is related to the volume of the sample ($V$), the contrast between the two phases ($\rho_1 - \rho_2$), and the volume fractions of the two phases ($\phi_1$ and $\phi_2$). This relationship allows the interpretation of changes in morphology in some materials. In this case, the scattering length densities (SLDs or $\rho$) of the homogeneous material are starting to change as the material reorganizes. The SLD of the regions that are becoming more organized is increasing, generating increased contrast and leading to an increase in the scattering power ($Q$) of the sample. By calculating $Q$, one can obtain a measure of the densification of the regions in which crystallites are nucleating.

Figure 4 shows the results of the invariant analysis. In the first 15 h, approximately, the invariant increased from 78 to 87.5 units. From 15 h to the end of the experiment at 103 h, the invariant continued to increase but a slower rate. At the end of the experiment, the invariant reaches an average value of 93 × $10^{-7}$ units (mol $e^{-2}cm^{-3})^3$. Importantly, no obvious change in the rate of increase in $Q$ is observed at the end of the experiment, suggesting that $Q$ would continue to increase with time.

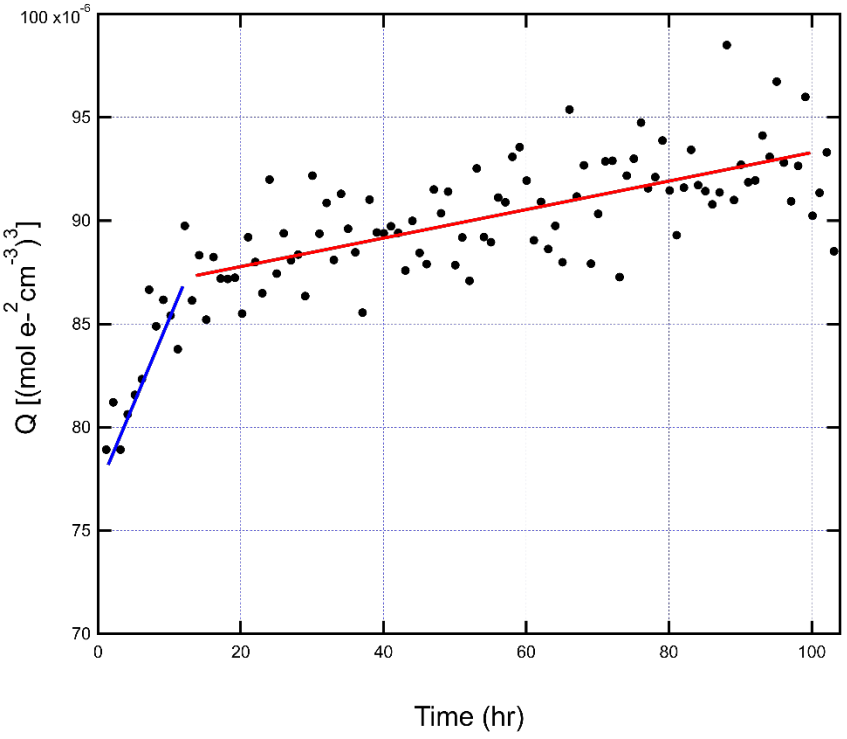


**Fig. 4 Invariant calculated from SAXS data collected from PPS annealed at 70 °C. Solid lines are provided as guides only. Note that the y-axis is not full scale.**

Based on Eq. 1, one can interpret the data in Fig. 4 as an increase in contrast ($\rho_1 - \rho_2$), a change in the volume fraction of the crystalline phase, or both. Given that no crystallites are present below $T_m$, it is not appropriate to consider the SLD of the densifying phase ($\rho_2$) as fixed at the SLD of the crystallites. It is also not appropriate to consider the volume fraction of the crystalline phase ($\phi_2$) as fixed. With the two dependent parameters defining the second phase changing simultaneously, it is not possible to quantify either separately. However, it is reasonable to conclude that both are increasing from zero, when the sample is uniformly amorphous with no small-angle scattering (i.e., at time = 0). The morphology of the PPS sample begins changing immediately when held at 70 °C and changes continuously through the first 103 h of annealing. The immediate change observed suggests that PPS will be unstable at even lower temperatures, with instability taking longer to manifest at cooler temperatures.

## 3.3 Polycarbonate

The PC material characterized was actually a copolymer of PC and siloxane, primarily poly(dimethyl siloxane) (PDMS), a soft, viscoelastic material most likely added to improve toughness. Neat PC is an amorphous polymer with a $T_g$ of 147 °C and therefore expected to be largely featureless in SAXS and WAXS characterization.

Figure 5A shows the combined SAXS and WAXS scattering data for the PC-siloxane material, from 20 to 200 °C. Although the WAXS portion of the data is generally featureless other than the expected amorphous halo (around 1.1 $Å^{-1}$), the SAXS regime shows a large feature peak that is not fully revealed in the data from Fig. 5A. Figure 5B shows the SAXS data collected for the same PC-siloxane sample when heated from 20 °C to 200 °C. The SAXS data are dominated by a large peak centered about 0.0135 $Å^{-1}$, corresponding to a real-space dimension of 46.5 nm. The presence of this feature indicates the presence of a two-phase morphology of microphase-separated domains comprising the “siloxane” additive.

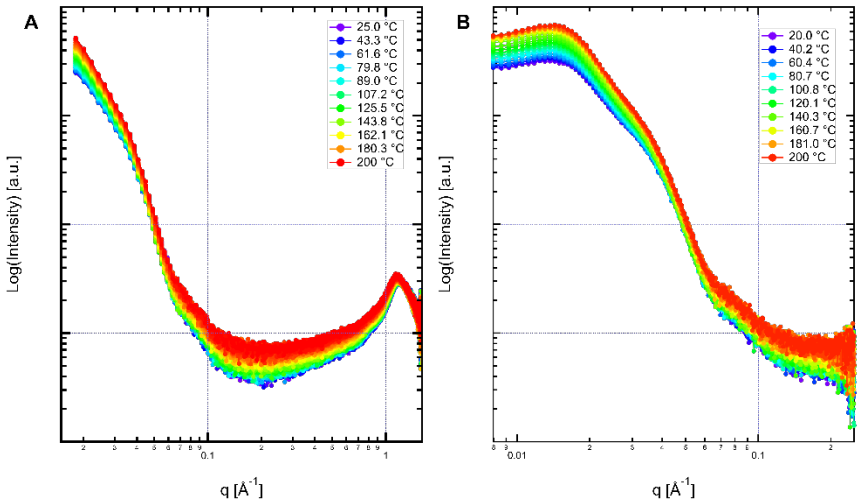


**Fig. 5 A) Combined SAXS and WAXS data for PC-siloxane copolymer collected from 20 to 200 °C. B) SAXS data for PC-collected from 20 to 200 °C.**

A direct fit to the SAXS data using a form factor and structure factor was not possible. However, using the Maximum Entropy method,[17] a particle size distribution was extracted assuming spherical domains, as shown in Fig. 6. The Maximum Entropy method creates a scattering curve that is the sum of weighted individual contributions for domains that have sizes defined by the size distribution curve. As a result, it does not account well for interparticle scattering. This is true of the data in Fig. 6, where at low angles the model fit (blue) deviates visibly from the scattering data (black). The normalized residual also shows this deviation. However, the residuals are lower at intermediate and higher angles, suggesting that particle size distribution is of more value for the smaller particle sizes. The distribution has a mean particle diameter of 17.4 nm, a median diameter of 16.6 nm, and a radius of gyration of 8.9 nm. The suggests the presence of 17-nm-diameter PDMS domains with an average spacing between domains of roughly 47 nm. The PDMS domains are too small to scatter light, consistent with the transparent and featureless material.

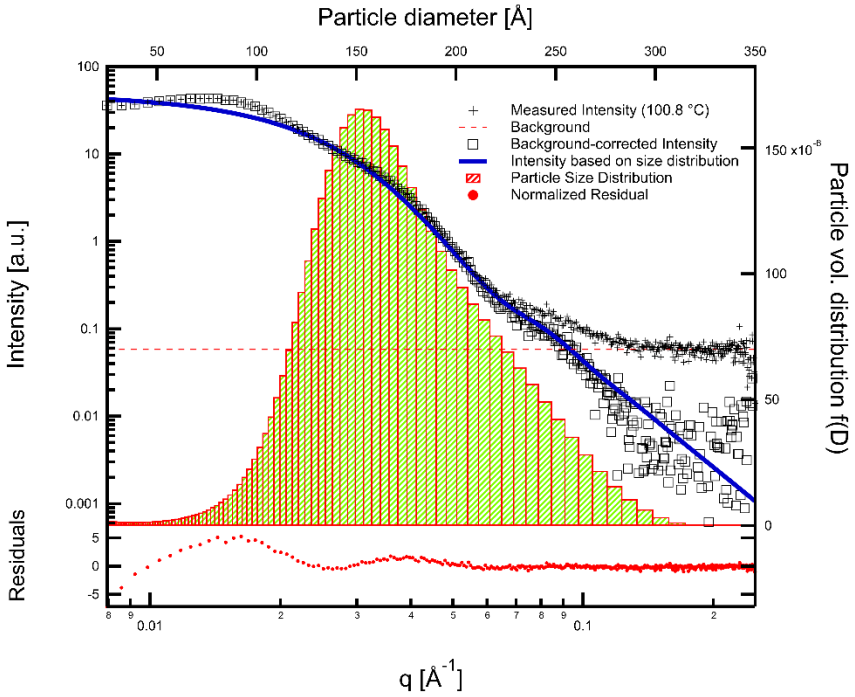


**Fig. 6 Results of the Maximum Entropy analysis of particle size distribution when applied to the SAXS data for PC-siloxane measured at 100.8 °C. The fit to the measured data is shown in blue, while the particle size distribution curve is in green and red.**

The only change in the SAXS or WAXS data with increasing temperature is an increase in the scattered intensity with temperature, as can be seen in Fig. 5. The origin of this increase, which is uniform across all length scales, is unclear. Thermal diffuse scattering, which increases with temperature, is generally associated with wide-angle scattering because it pertains to vibration-induced displacement of atoms from their normal positions—length scales two or more orders of magnitude smaller than in the SAXS regime. The consistency of the increased scattering, which is a factor of approximately 2 over the entire range of the SAXS data, suggests that it is due to a factor that is not a function of angle. A change in sample volume could produce this effect, as measured intensity is directly proportional to the volume of material characterized.[2] The coefficient of thermal expansion of PC is only $7.0 \times 10^{-5}$/°C, which would give a linear expansion of 1.3% in 180 °C. However, stress relaxation can result in significant changes in sample volume, especially if the material is trapped in a highly nonequilibrium state (e.g., drawn and quenched). Dramatic stress relaxation of this type was visually observed in PC-siloxane samples analyzed by dynamic mechanical analysis as a part of a larger research effort with these materials. Regardless of origin, this effect is not directly relevant to the overall goal of this study. Here, the PC-siloxane morphology appears to be stable.

## 3.4 Poly(phenyl sulfone)

PPSU is thought to be a good candidate for thermal stability, having both a high $T_g$ (220 °C) and a high heat-deflection temperature (207 °C). The WAXS data in Fig. 7 show only the amorphous halo at any temperature considered. The halo itself does shift slightly to lower *q*, but this is due to a slight increase in interchain spacing due to thermal motion and does not reflect a change in morphology.

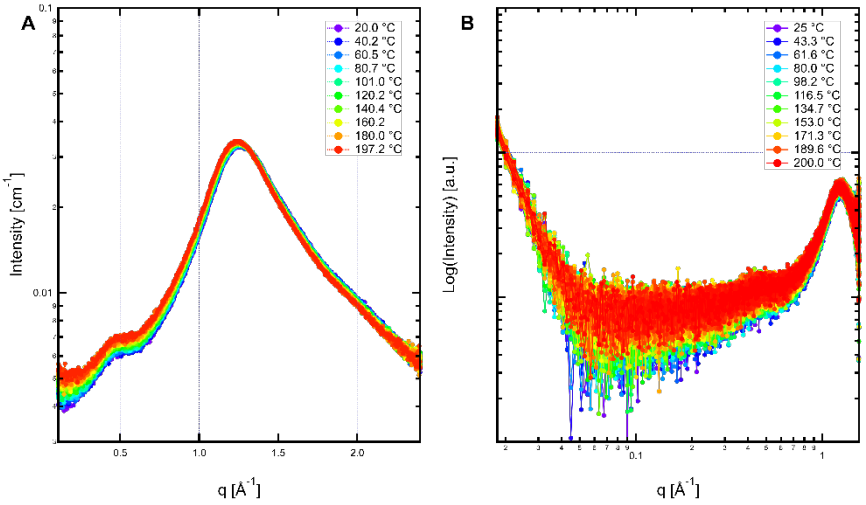


**Fig. 7 A) WAXS data collected for the PPSU material, spanning a temperature range from 20 to 200 °C. No evidence of crystallinity or melting is observed. B) Combined SAXS and WAXS data collected at 200 mm with detector offset. No changes in morphology are observed.**

As in the PC-siloxane sample, there again appears to be an increase in the SAXS scattering intensity, observed in the lowest *q* portion of Fig. 7A, from 0.5 $Å^{-1}$ and lower. Curiously, this is not observed in the data shown in Fig. 7B, which were collected at an intermediate SDD to allow simultaneous capture of SAXS and WAXS data in one measurement. However, unlike the PC-siloxane material, which had clear structure in the SAXS regime, there is virtually no scattering from PPSU in this region, making a direct comparison difficult. Also visible in the SAXS data is a very weak polymerization peak at approximately 0.5 $Å^{-1}$. Polymerization peaks are produced by scattering length density variations along the polymer backbone.[18] In this case, the repeating sulfone structure is the most likely origin. A change in the position of the polymerization peak would not be expected from a change in temperature unless the chemical structure somehow changed.

Therefore, again the SAXS and WAXS data show that there is no morphological change in the PPSU observed between 20 and 200 °C, making this material a strong candidate for high-temperature applications.

## 3.5 Poly(ether imide)

PEI is another strong candidate for a high-temperature application, with a heat-deflection temperature of 201 °C and a $T_g$ of 215 °C.[9] SAXS and WAXS data collected for PEI are shown in Fig. 8. In both cases, behavior virtually identical to that of the PPSU is observed. In the WAXS regime, only an amorphous halo is observed, and, as with any polymer, shifts to slightly lower angles with increased molecular motion enabled by elevated temperature. In the SAXS data, the only feature observed is a polymerization peak at approximately 0.45 $Å^{-1}$. This feature most likely arises from the repeating imidazole moiety in the PEI molecules. A further SAXS data set was collected at room temperature (not shown) and showed no morphological features. This absence of features and changes in the few features observed makes PEI also a good candidate material.

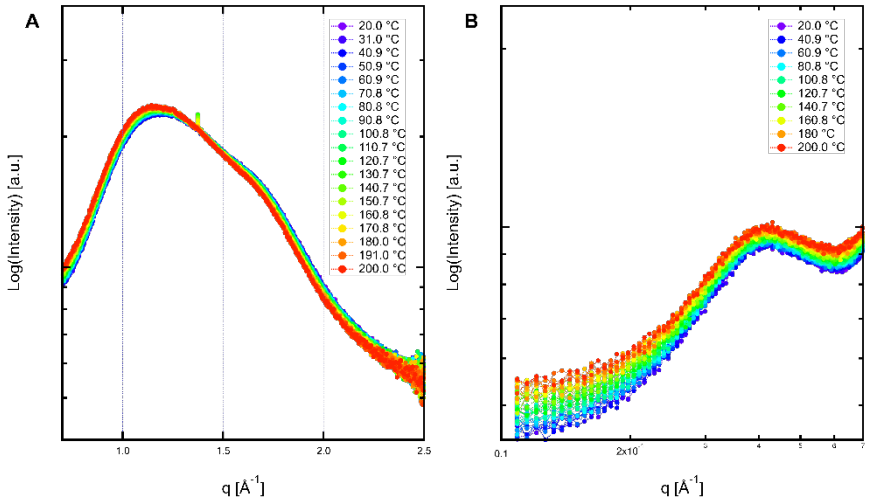


**Fig. 8 A) WAXS data collected from 20 to 200 °C for PEI. No change in morphology is observed, and only a slight change in the position of the amorphous halo due to increased molecular motion. The sharp peak at 1.35 $Å^{-1}$ is thought to be from a defect in a mica window. B) SAXS data collected from PEI between 20 to 200 °C. Only a polymerization peak is observed.**

## 3.6 High-Temperature Nylon

Two final materials were studied. These were "high-temperature nylons," both with glass-fiber filler (HTN-F) and impact modified (HTN-IM). Both of these materials are polyphthalamides (PPAs), a subset of polyamide materials (i.e., nylons). PPAs incorporate terephthalic and isophthalic copolymers to increase the aromatic character of the material, resulting in an increased $T_g$, $T_m$, and modulus relative to more common aliphatic grades of nylon. Unmodified nylon-6,6 melts at 325 °C and has a HDT of 125 °C.

Figure 9A shows WAXS data collected for HTN-IM at both 20 and 200 °C, data that both show weak Bragg diffraction peaks superimposed on the amorphous halo between 1.2 and 1.8 $Å^{-1}$. Heating the sample to 200 °C causes the diffraction peaks to sharpen noticeably, although they still are relatively weak. This indicates that the crystallites are becoming better ordered internally but are not increasing in size or number—behavior consistent with annealing substantially below $T_m$. Figure 9B shows the WAXS data collected from the HTN-F sample at 23 and 275 °C. Notably, the maximum temperature for HTN-F was raised to observe any response in the sample, which was remarkably stable over the temperature range up to 200 °C. Unlike HTN-IM, the diffraction peaks observed at 275 °C are not markedly improved from the room temperature data although they are slightly different. This may be due to the higher temperature or possibly to the presence of the glass fiber filler material, which would impede molecular motion even above $T_m$.

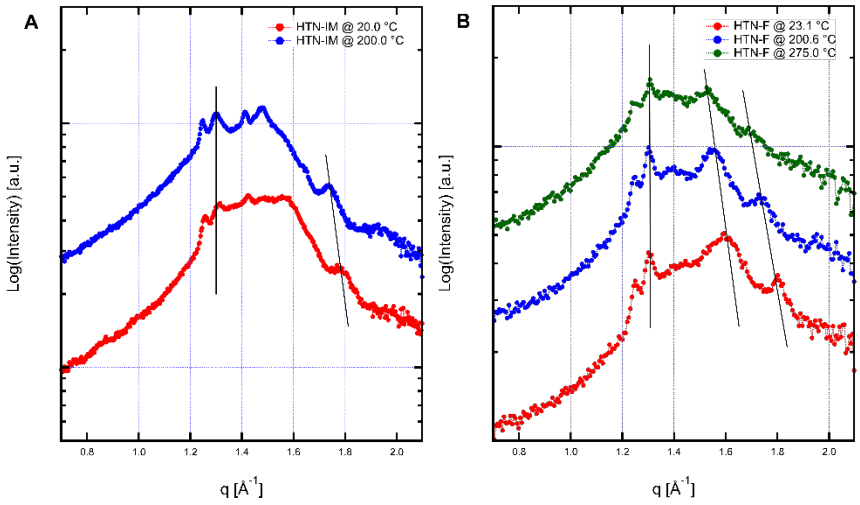


**Fig. 9 A) WAXS data for HTN-IM at 20 and 200 °C. The diffraction peaks are better defined at 200 °C, indicating that the crystalline structure is improving with annealing. B) WAXS data at 23, 200.5, and 275 °C for HTN-F, scaled vertically for clarity. The solid lines indicate relative changes in specific diffraction peaks with temperature.**

Figure 10 shows the effect of heating to 200 °C on both the filled and the unfilled HTN materials. For both polymers, the SAXS feature centered at 0.06 $Å^{-1}$ increases in intensity and definition with increasing temperature. This corresponds well with the observed changes in the weak diffraction peaks in Fig. 9. As the crystallites improve slightly in definition, the contrast between the matrix and crystalline regions can be expected to increase slightly. Slight changes to the shape of the crystalline domains would also be anticipated to affect the form factor scattering observed in SAXS. The changes are similar to that observed from PPS (Fig. 3) in that the intensity of the feature increases initially and is virtually identical to the behavior observed for HTN-IM (Fig. 10). As in the case of PPS (see Fig. 2B), the onset of this morphological change at temperatures around 100 °C is concerning.

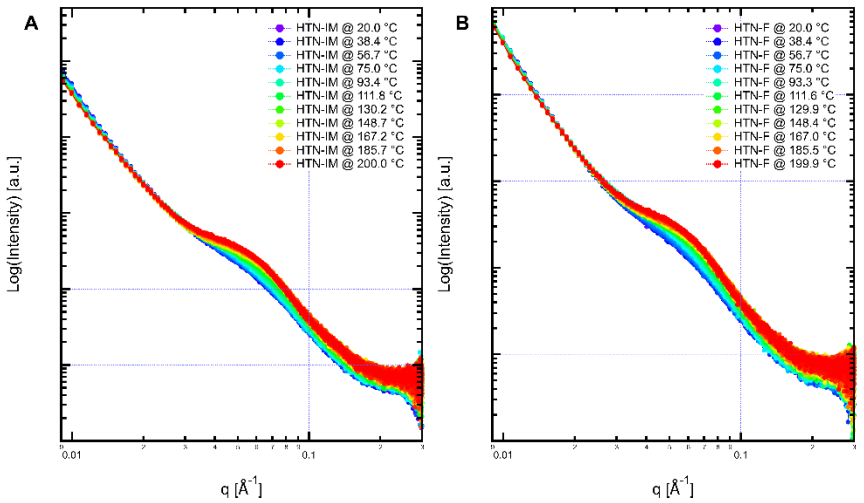


**Fig. 10 SAXS data from 20 to 200 °C for A) HTN-IM and B) HTN-F. The low-angle feature arising from the poorly defined crystallites increases in intensity with temperature, suggesting a small improvement in crystallite definition.**

## 4. Summary and Conclusion

In this study, X-ray scattering was combined with in situ heating to explore the morphological stability of a series of thermoplastics typically used in high-temperature applications. Samples of commercial products were heated during SAXS and WAXS measurements from room temperature to at least 200 °C. Lexan 1414T, a proprietary blend based primarily on PC and a poly(siloxane), PPSU, and the PEI products tested showed the best thermal stability. The PPSU and PEI materials exhibited very little morphological information and remained completely unstructured and amorphous through the temperature range. The Lexan sample presented a small-angle feature that suggests microphase separation due to the addition of the siloxane component, but also showed no substantive changes in morphology with temperature. In contrast, samples of POM, PPS, HTN-IM, and HTN-F exhibited changes in morphology as a function of temperature. POM exhibited strong crystallinity at room temperature and displayed a sharp melting transition around 170 °C, becoming a free-flowing liquid. The SAXS data indicate that the POM crystallites begin to change as early as 130 °C. In contrast, PPS crystallized upon heating at approximately 105 °C. Importantly, PPS was found to be morphologically unstable at only 70 °C with measurable changes in the low-*q* scattering. Calculations of the Porod Invariant indicate that annealing at 70 °C produces a relatively rapid increase in scattering followed by continued change at a slower rate. After 100 h of annealing, the PPS morphology was still evolving. This change is due to the onset of localized density fluctuations that eventually allow the development of crystallites and can be expected to affect physical

properties. These results suggest that PPSU, PEI, and the PC-siloxane product studied here may be considered thermally stable under these testing conditions.

## 5. References


1. Glatter O, Kratky O. Small angle X-ray scattering. Academic Press; 1982.
2. Roe R-J. Methods of X-ray and neutron scattering in polymer science. Oxford University Press; 2000.
3. Bras W, Ryan AJ. Sample environments and techniques combined with small angle X-ray scattering. Adv Colloid Interface Sci. 1998;75(1):1–43. doi: 10.1016/s0001-8686(97)00032-8.
4. Elwell MJ, Ryan AJ, Grunbauer HJM, VanLieshout HC. In-situ studies of structure development during the reactive processing of model flexible polyurethane foam systems using FT-IR spectroscopy, synchrotron SAXS, and rheology. Macromolecules. 1996;29(8):2960–2968. doi: 10.1021/ma9511208.
5. Somani RH, Hsiao BS, Nogales A, Srinivas S, Tsou AH, Sics I, Balta-Calleja FJ, Ezquerra TA. Structure development during shear flow-induced crystallization of i-PP: in-situ small-angle X-ray scattering study. Macromolecules. 2000;33(25):9385–9394. doi: 10.1021/ma001124z.
6. Lambeth RH, Morgan BF, Savage AM, Beyer FL. Metallo-supramolecular crosslinked polyurethanes. J Polym Sci Part B Polym Phys. 2019;57(24):1744–1757. doi: 10.1002/polb.24909.
7. Nogales A, Hsiao BS, Somani RH, Srinivas S, Tsou AH, Balta-Calleja FJ, Ezquerra TA. Shear-induced crystallization of isotactic polypropylene with different molecular weight distributions: in situ small- and wide-angle X-ray scattering studies. Polymer. 2001;42(12):5247–5256. doi: 10.1016/S0032-3861(00)00919-8.
8. Janarthanan R, Horan JL, Caire BR, Ziegler ZC, Yang Y, Zuo XB, Liberatore MW, Hibbs MR, Herring AM. Understanding anion transport in an aminated trimethyl polyphenylene with high anionic conductivity. J Polym Sci Part B Polym Phys. 2013;51(24):1743–1750. doi: 10.1002/polb.23164.
9. Sastri VR. High-temperature engineering thermoplastics: polysulfones, polyimides, polysulfides, polyketones, liquid crystalline polymers, and fluoropolymers. In: Sastri VR, editor. Plastics in medical devices. 2nd ed. William Andrew Publishing; 2014. p. 173–213. Chapter 8.
10. Ivan'kova EM, Vaganov GV, Popova EN, Elokhovskiy VY, Kasatkin IA. Structure-property relationship of polyetherimide fibers filled with carbon nanoparticles. ACS Omega. 2020;5(19):10680–10686. doi: 10.1021/acsomega.9b04102.

11. Huang TC, Toraya H, Blanton TN, Wu Y. X-ray-powder diffraction analysis of silver behenate, a possible low-angle diffraction standard. J Appl Crystallogr. 1993;26:180–184.

12. Ilavsky J. Nika: software for two-dimensional data reduction. J Appl Crystallogr. 2012;45:324–328. doi: 10.1107/s0021889812004037. Ilavsky J, Jemian PR. Irena: tool suite for modeling and analysis of small-angle scattering. J Appl Crystallogr. 2009;42:347–353.

13. Brandrup J, Immergut EH, Grulke EA. Polymer handbook. 4th ed. John Wiley and Sons; 1999. p. 2366.

14. Tadokoro H. Structure of crystalline polymers. Robert E Krieger Publishing Company; 1979.

15. Chen TL, Sun R, Willis C, Krutzer B, Morgan BF, Beyer FL, Han KS, Murugesan V, Elabd YA. Impact of ionic liquid on lithium ion battery with a solid poly(ionic liquid) pentablock terpolymer as electrolyte and separator. Polymer. 2020;209:12. doi: 10.1016/j.polymer.2020.122975.

16. Beyer FL, Masser KA, Lenhart JL. Application of the small-angle scattering invariant to morphological behavior in ballistic materials. J Appl Polym Sci. 2021;138(21):50478. doi: 10.1002/app.50478.

17. Morrison JD, Corcoran JD, Lewis KE. The determination of particle-size distributions in small-angle scattering using the maximum-entropy method. J Appl Crystallogr. 1992;25:504–513. doi: 10.1107/s0021889892001729.

18. Mitchell GR, Windle AH. Structure of polystyrene glasses. Polymer. 1984;25 (7):906–920. https://doi.org/10.1016/0032-3861(84)90073-9.

## List of Symbols, Abbreviations, and Acronyms

| | |
|---|---|
| λ | wavelength |
| $\rho$ | SLD, or scattering length density |
| $\varphi$ | volume fraction |
| 1-D | one-dimensional |
| 2-D | two-dimensional |
| Af | method **A**, **f**lat orientation |
| HTN-IM | impact-modified high-temperature nylon |
| HTN-F | filled high-temperature nylon |
| HDT | heat-deflection temperature |
| PC | poly(carbonate) |
| PDMS | poly(dimethyl siloxane) |
| PEI | poly(ether imide) |
| POM | poly(oxymethylene) |
| PPA | poly(phthalimide) |
| PPS | poly(p-phenylene sulfide) |
| PPSU | poly(phenyl sulphone) |
| $q$ | scattering vector magnitude |
| $Q$ | Porod Invariant |
| SAXS | small-angle X-ray scattering |
| SDD | sample-to-detector distance |
| SLD | scattering length density |
| $T_g$ | glass transition temperature |
| $T_m$ | glass melting temperature |
| $V$ | sample volume |
| WAXS | wide-angle X-ray scattering |

| | |
|---|---|
| 1 (PDF) | DEFENSE TECHNICAL INFORMATION CTR DTIC OCA |
| 1 (PDF) | DEVCOM ARL FCDD RLD DCI TECH LIB |
| 2 (PDF) | DEVCOM ARL FCDD RLW MG F BEYER R MROZEK |